International Journal of Greenhouse Gas Control 99 (2020) 103055

Contents lists available at ScienceDirect

International Journal of Greenhouse Gas Control

journal homepage: www.elsevier.com/locate/ijggc

Optimization and comparison of the two promising oxy-combustion cycles NET Power cycle and Graz Cycle

Kevin Wimmer, Wolfgang Sanz*

Graz University of Technology, Institute for Thermal Turbomachinery and Machine Dynamics, Inffeldgasse 25, Graz, 8010, Austria

ARTICLE INFO

Keywords:
Oxy-fuel combustion
CO_2 capture and storage
Graz Cycle
NET Power cycle
Thermodynamic analysis
Cycle optimization

ABSTRACT

Carbon capture and storage (CCS) is considered an effective measure to reduce the anthropogenic CO_2 emissions. Oxy-combustion with a theoretical capture rate of 100% is a very promising CCS technology. In order to show the potential of oxy-combustion two highly-efficient power cycles, the NET Power cycle and the Graz Cycle, are thus thermodynamically optimized and compared at full load for firing with natural gas.

The simulation of both cycles is carried out using the thermodynamic simulation software IPSEpro. Particular attention is paid to provide the same boundary conditions and assumptions for both processes to ensure a correct comparison. As a starting point a base case for each cycle is simulated based on the literature data. Both power cycles are then optimized by varying the main cycle parameters using a genetic algorithm. The optimized processes show a slightly higher net efficiency considering oxygen supply and CO_2 compression for the Graz Cycle with 53.5% compared to 52.7% for the NET Power cycle. Moreover, the main differences of both cycles are discussed and the impact of assumptions of component losses and efficiencies as well as the minimum cycle temperature on both cycles is discussed.

1. Introduction

Research data and many climate indicators reveal that climate change is taking place, and the majority of politicians and scientists are convinced that this is connected to the anthropogenic emission of greenhouse gases, mainly CO_2. The report "State of the Climate in 2017" of the National Oceanic and Atmospheric Administration (NOAA) states that in 2017 the dominant greenhouse gases released into Earth's atmosphere—carbon dioxide, methane, and nitrous oxide—reached new record highs and that the ten warmest years on record have all occurred since 1998, with the four warmest years occurring since 2014 (Hartfield et al., 2018).

Taking into consideration a further increase of the world population and an increasing standard of living in the developing countries, energy consumption will also rise. Without changes in energy policy this might lead to more CO_2 emissions which would accelerate climate change.

Restricting the threats of climate change will be one of the most demanding challenges for the future. The primary objective is the reduction of CO_2 emissions, which are mainly caused by burning fossil fuels. There are mainly four options for reducing these emissions:

- increasing the efficiency of energy use
- using renewable energies
- carbon dioxide capturing and storage (CCS)
- using nuclear energy for power generation (Fischedick et al., 2015)

CCS is a promising mid-term solution for reducing CO_2-emissions. In the World Energy Outlook 2016 (WEO 2016) the International Energy Agency (IEA) investigated a scenario for limiting the average global temperature increase in 2100 to 2 degrees Celsius above pre-industrial levels, where 8% of the electricity should be produced by CCS (International Energy Agency, 2016).

One promising CCS technology for power generation is oxy-fuel combustion. The fossil fuel is burned with almost pure oxygen, so that the flue gas occurring consists mainly of CO_2 and water steam. By cooling the flue gas most of the water steam condenses and can be easily separated from CO_2. The necessary oxygen is mainly provided by a cryogenic air separation unit (ASU). Two oxy-fuel combustion cycles, which showed promising efficiencies in former investigations are the Graz Cycle (GC) and the NET Power cycle (NC).

NET Power presented its oxy-fuel power cycle with promising efficiencies first in (Allam et al., 2011). Further thermodynamic analysis, a parameter study and optimization of the cycle were conducted by (Scaccabarozzi et al., 2016, 2017). Currently the NC is tested at a demonstration plant in La Porte, Texas (Allam et al., 2017).

The basic principle of the GC was developed by H. Jericha in 1985

* Corresponding author.
E-mail address: wolfgang.sanz@tugraz.at (W. Sanz).

https://doi.org/10.1016/j.ijggc.2020.103055
Received 20 November 2019; Received in revised form 5 March 2020; Accepted 20 April 2020

(Jericha, 1985). Many further developments for the GC have been presented since then (Jericha et al., 1995, 2006, 2008; Sanz et al., 2004, 2005, 2008).

So far, only one comparison of the two cycles under similar boundary conditions and assumptions has been carried out (IEAGHG, 2015). This report showed an advantage in the net efficiency of 5.7% points for the NC compared to the GC. But the study is based on different thermodynamic simulation codes as well as assumptions on fluid properties, which were necessary because of the very different working fluids. So for the NC Aspen Plus v7.3 with a cooled gas turbine model based on (El-Masri, 1986) was used and the working fluid consisting mainly of CO_2 was modelled with the Peng-Robinson real gas model (Peng and Robinson, 1976). For the GC the GS code developed at Politecnico di Milano was applied with the cooled expansion model by (Chiesa and Macchi, 2004). The thermophysical properties of the working fluid were evaluated as an ideal mixture of ideal gases, but with water and steam treated as real fluid. The authors made great efforts to calibrate their models and assumptions to put their comparison on a common basis but there are still some uncertainties.

In this work a thermodynamic comparison of these two promising oxy-fuel cycles was thus performed using the same simulation code (IPSEpro v7 by SIMTECH Simulation Technology (SimTech Simulation Technology, 2017)), the same cooled turbine model (developed in (Sanz et al., 2005)), the same equation-of-state models for the working fluids and similar component efficiencies and losses for both cycles. By this means an answer shall be provided for the question of whether the conclusions on cycle quality drawn from (IEAGHG, 2015) are independent of the used simulation tool and models as well as of the applied assumptions on fluid properties. In terms of the NET Power cycle the work of (Scaccabarozzi et al., 2016) is used as basis for the comparison because they revised the NET Power cycle as designed in (IEAGHG, 2015). The study shall also provide information on the sensitivity of thermodynamic studies on the chosen assumptions by performing an additional parameter study and an optimization for both cycles.

2. Description of the NET Power cycle and the Graz Cycle

2.1. NET Power cycle

In this work the NC is operated with natural gas (gasified solid fuels as coal or biomass could also be used). The natural gas is fired with almost pure oxygen. The flue gas of the NC consists mainly of CO_2 and only small amounts of water, because of water separation before recirculation. In addition the gas also contains small quantities of oxygen (O_2), nitrogen (N_2) and Argon (Ar).

Fig. 1 presents a principle flow scheme of the Net Power cycle and Fig. 2 provides a temperature-entropy (T–s) diagram. The flow sheet used for the thermodynamic simulation can be found in the appendix (Fig. 21) and gives mass flow, pressure, temperature and enthalpy of all streams. Natural gas and two recycled CO_2-streams enter the combustion chamber coming from the recuperator (point 6 in T–s diagram). The left oxidant stream (dark red) also contains oxygen stemming from the air separation unit (ASU). The working fluid with a composition of 96% CO_2 and 2.7% H_2O exits the combustion chamber with a temperature above 1100 °C and a pressure of around 300 bar (point 1). In the downstream high-pressure turbine this is expanded to around 35 bar and 750 °C (point 2). Cooling is done with a further recycled CO_2 stream. The heat of the turbine exhaust gas is used in the recuperator to heat the recycle stream and the oxidant stream. Further heat for the recuperator is gained from the ASU as its main compressor generates air with 270 °C if it is not intercooled. Although this increases the power consumption of the ASU, according to the cycle developers (Allam et al., 2013) the overall effect on the cycle efficiency is positive.

After the recuperator the cycle fluid has a temperature of around 50 °C (point 3) and by further cooling in the condenser water condenses and can be separated (point 4). A small amount of the almost pure CO_2, which corresponds to the combustion generated CO_2, is removed from the cycle, sent to the compression and purification unit (CPU) and supplied for further use or storage. The major part is compressed to 80 bar and 26 °C by four intercooled compressors (recycle flow compressors). Further condensed water is removed from the intercoolers. At this condition the cycle fluid is supercritical with the advantage of high densities at low viscosities. This is beneficial in terms of the power needed for the following compression to 300 bar which can be achieved using pumps.

The cycle fluid is first pumped to 120 bar and then split in front of the recuperator into what are known as the recycle stream and the oxidant stream. The recycle stream is compressed to 300 bar (point 5) and then split into two streams. The major part is heated to 720 °C in the recuperator and sent to the combustion chamber, the other part is also heated in the recuperator, but to lower temperatures and serves as cooling for the turbine. The oxidant stream is mixed with almost pure oxygen (99.5% purity, molar basis) from the ASU and subsequently compressed to 300 bar and also heated to 720 °C in the recuperator. The mixing of the CO_2 with the oxygen occurs at 120 bar, because the ASU is limited to this pressure.

The temperature-entropy (T–s) diagram in Fig. 2 gives a good overview of the thermodynamic characteristics of the NC. As the cycle fluid contains mainly CO_2, the saturation curve is plotted for CO_2. The two positive characteristics of the NC are the supercritical compression with pumps to point 5 and the high recuperation with heat transferred from the hot turbine exhaust flow (point 2 to 3) to heat up the compressed cycle fluid from point 5 to 6. Moreover, a share of the power consumed by the ASU can be recovered by transferring cooling heat of the main compressor to the recuperator.

2.2. Graz Cycle

The Graz Cycle is also suited for all kinds of gaseous fossil fuels, but in this work it is fired with natural gas. The combustion with almost pure oxygen (from an ASU) and the recycling of the water leads to a working fluid consisting of around three quarters of water and one quarter of CO_2.

Fig. 3 shows the principle flow scheme of the GC as presented in (Sanz et al., 2005) and Fig. 4 the associated T–s diagram (as the composition of the cycle fluid varies, the saturation curve is only plotted for H_2O). The flow sheet used for the thermodynamic simulation of the Graz Cycle can be found in the appendix (Fig. 22) and gives mass flow, pressure, temperature and enthalpy of all streams. The Graz Cycle consists basically of a high temperature Brayton cycle (compressors C1 and C2, combustion chamber and High Temperature Turbine HTT) and a low temperature Rankine cycle (Low Pressure Turbine LPT, condenser, Heat Recovery Steam Generator HRSG and High Pressure Turbine HPT).

The fuel together with the nearly stoichiometric mass flow of oxygen is fed to the combustion chamber, which is operated at a pressure of 40 bar. Steam as well as a CO2/ H_2O mixture is supplied to cool the burners and the liner. The working fluid leaves the combustion chamber with a temperature of around 1400 °C and a pressure of 40 bar (point 1 in the T–s diagram of Fig. 4). In the High Temperature Turbine (HTT) the working fluid is expanded to 1.05 bar and 579 °C (point 2). Cooling is performed with steam coming from the HPT at about 330 °C (13.7% of the HTT inlet mass flow), further increasing the steam content from 74% at combustor exit to 76% at the HTT exit. The hot exhaust gas is then cooled in the following HRSG to vaporize and superheat steam for the HPT.

But after the HRSG the working fluid is divided into two streams (point 3). About 55% of the cycle mass flow is further cooled in the HRSG (point 8) and compressed to 40 bar and a maximum temperature of 600 °C (point 9) by two intercooled compressors (C1/C2). It is then fed to the combustion chamber for cooling.

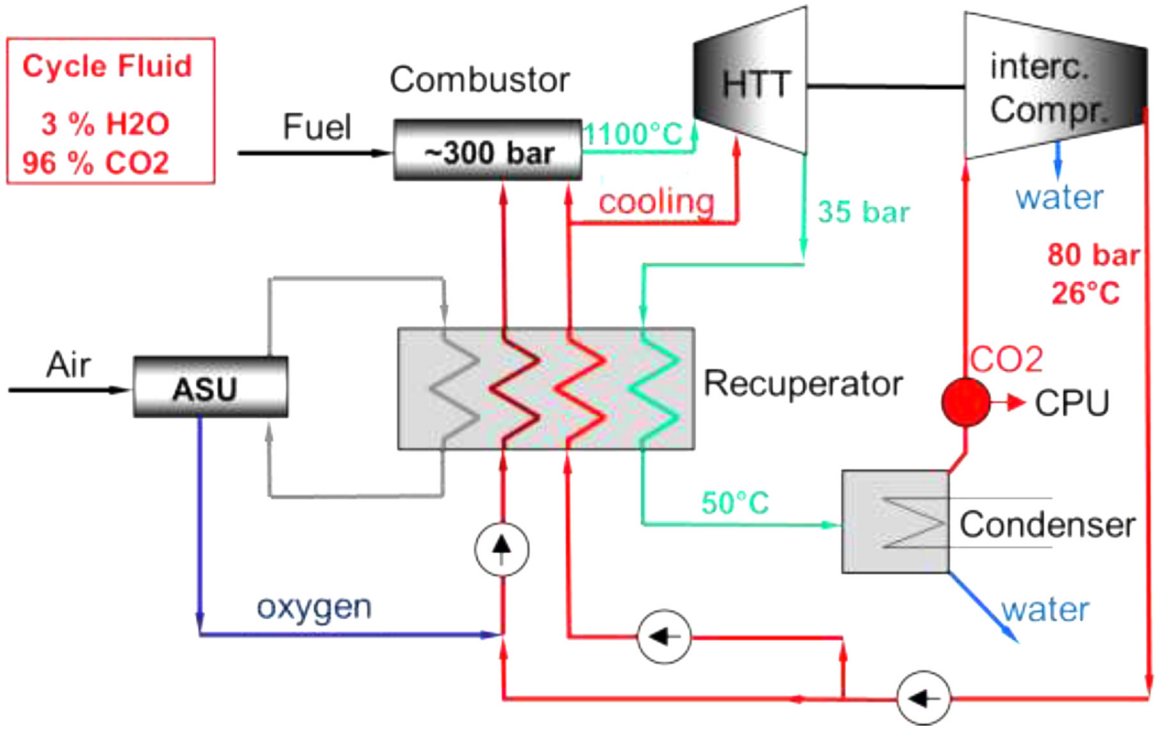

Fig. 1. Scheme of the NET Power cycle. (For interpretation of the references to color in this figure citation, the reader is referred to the web version of this article.)

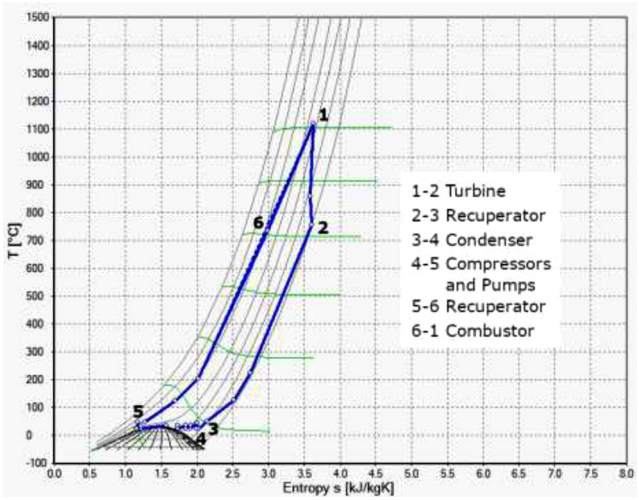

Fig. 2. Temperature-entropy diagram of the NET Power cycle.

The other part is further expanded to 0.04 bar (point 4) in the Low Pressure Turbine. The greater part of the water in the fluid condenses in the following condenser (point 5) and is separated. The gaseous part, which contains the combustion CO2 and half of the combustion water, is compressed to atmosphere by C3 and C4 with intercooling and further extraction of condensed combustion water. It is further compressed to 35 bar with the compressors C5 and C6 (not included in Fig. 3) and sent to the CPU and supplied for further use and storage.

The condensed water passes through a deaerator and is preheated, vaporized and superheated in the HRSG. The steam enters the High Pressure Turbine (HPT) with a temperature of 549 °C and a pressure of 180 bar (point 6). After the expansion through the HPT (point 7) the stream is used as cooling for the combustion chamber and the HTT.

The heat input at high temperatures (points 7 to 1 and points 9 to 1) as well as the expansion to very low pressures and temperatures (point 4) is beneficial for a high thermal efficiency according to Carnot. Furthermore, only a part of the steam in the cycle releases its heat in the condenser (points 4 to 5). The other part is compressed and sent back to the combustion chamber and thereby the heat is retained in the cycle.

3. Thermodynamic models and assumptions on main parameters

The thermodynamic analysis in this work is conducted with the program IPSEpro v7 from SIMTECH Simulation Technology (SimTech Simulation Technology, 2017). This software is used for modelling, analyzing and simulation of processes in power engineering.

3.1. Turbine model

A turbine model for the calculation of cooled turbine stages was developed in (Sanz et al., 2005). A simple stage-by-stage approach similar to (Jordal et al., 2003) is assumed which allows calculating the amount of cooling steam needed per stage. The module assumes that half of the cooling mass flow is mixed to the main flow at stage inlet, thus contributing to the stage expansion work. The rest is added at the stage exit.

For the cooled turbines in this investigation a maximum metal temperature of 860 °C and a temperature difference of 150 °C between the metal and cooling temperature at the cooling outlet to the main flow is assumed. Furthermore the surface ratio between cooled wall surface and flow passage is assumed with a value of 3. Further assumptions and details of the model are found in (Sanz et al., 2005).

3.2. Recuperator and heat recovery steam generator (HRSG) model

3.2.1. NET Power cycle

The heat transfer in the recuperator is relatively complex, since heat is exchanged between two hot streams (turbine outlet stream and ASU air stream) and three cold streams (oxidant stream, recycle stream and cooling stream) as illustrated in Fig. 5.

The turbine outlet stream enters the recuperator with a temperature of around 750 °C, the ASU air stream with a considerably lower temperature of 275 °C. The pinch-point of the recuperator occurs at that

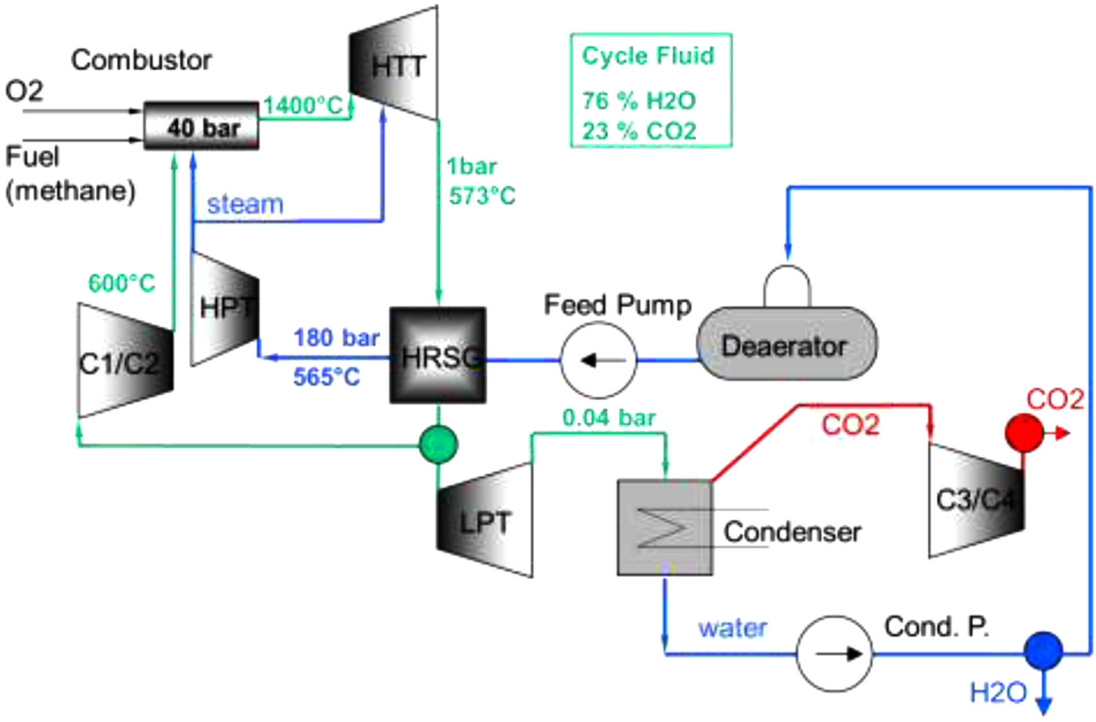

Fig. 3. Principle flow scheme of Graz Cycle power plant (Sanz et al., 2005).

point where water contained in the turbine outlet stream starts to condensate. Due to this complex situation the recuperator is modelled with three heat exchangers (HX1, HX2, HX3) as shown in Fig. 5.

At the inlet of the cold streams to HX1 the minimal allowed temperature difference is 5 °C. At the outlet where condensation starts the temperature difference is set to 5 °C. At the cold exit of HX2 and HX3 the temperature difference is set to 20 °C. The resulting temperature differences in the recuperator are demonstrated in the Q–T-diagram of Fig. 6.

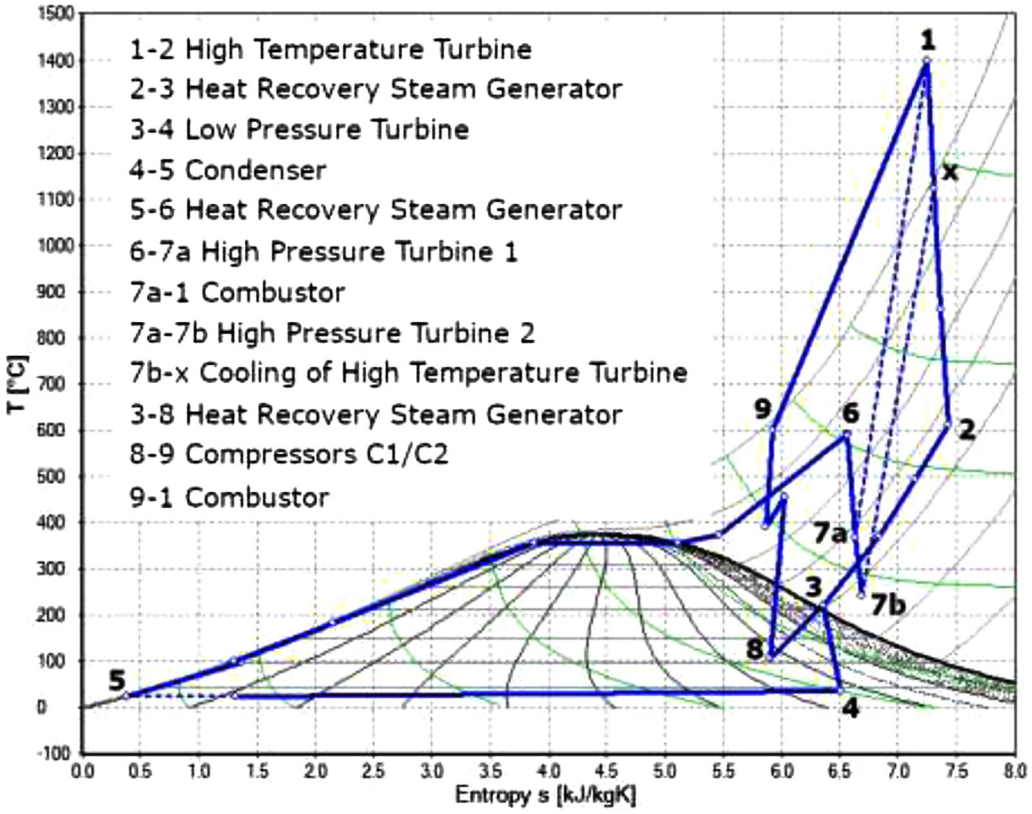

Fig. 4. Temperature-entropy diagram of the Graz Cycle.

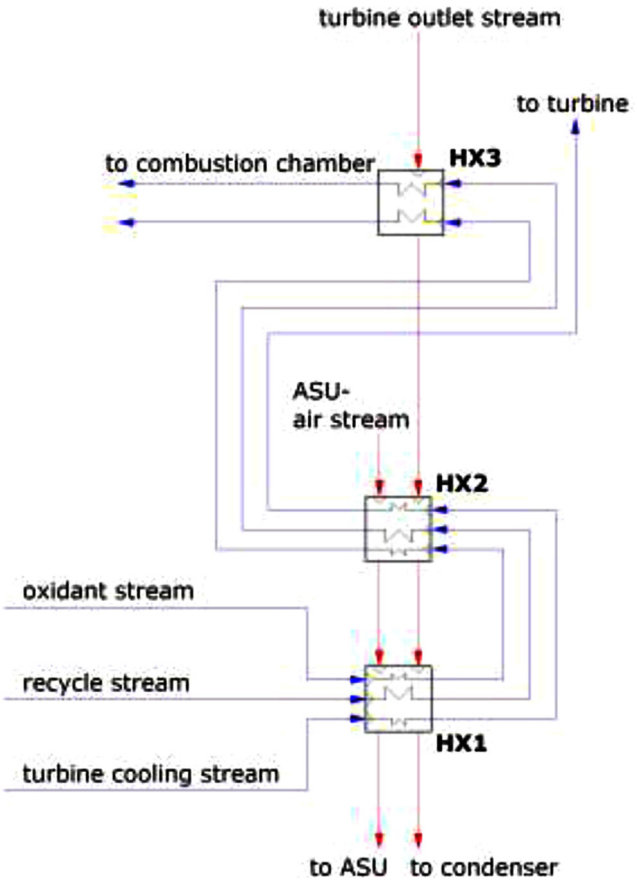

Fig. 5. Model of the recuperator (NC).

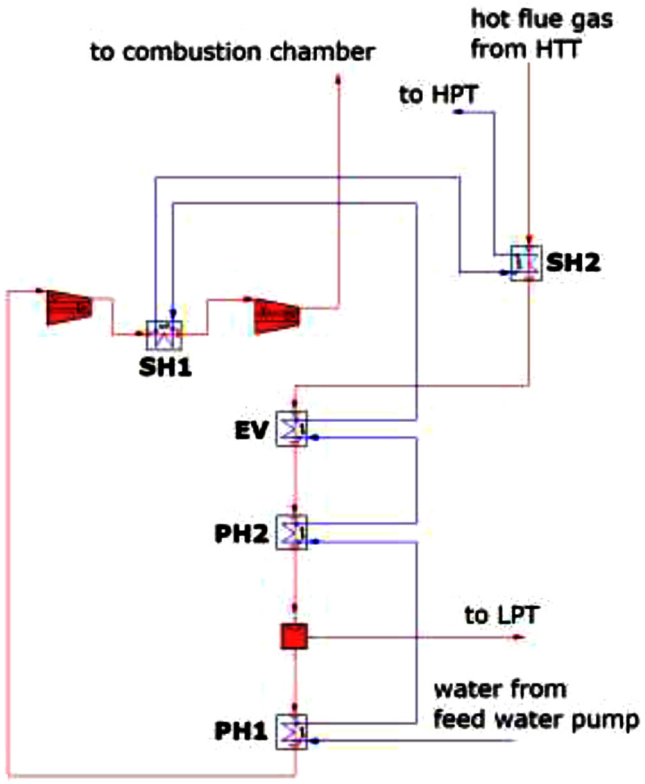

Fig. 7. Model of the HRSG (GC).

3.2.2. Graz Cycle

The HRSG consists of two preheaters (PH1 and PH2), one evaporator (EV) and two superheaters (SH1 and SH2) and is illustrated in Fig. 7. Heat is transferred from the hot flue gas to the cold water coming from the feed water pump.

SH1 is used to intercool the recycle compressors C1 and C2. The remaining heat exchangers are flown through by the flue gas of the HTT, whereby a part of the stream is diverted to the LPT in front of PH1. The water from the feed water pump passes through all five heat exchangers as in a standard steam process and exits as superheated steam. Fig. 8 gives the Q–T diagram of the heat transfer and shows the

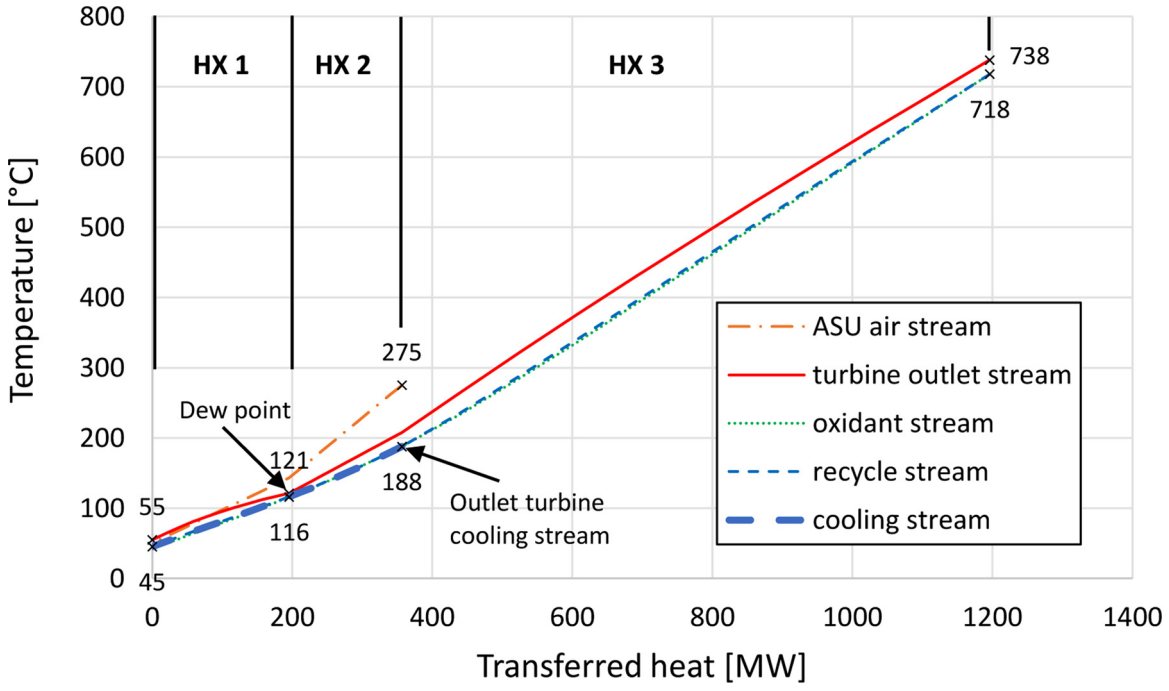

Fig. 6. Illustrative Q–T-diagram of the NET Power cycle; the lines for oxidant stream, recycle stream and cooling stream overlay.

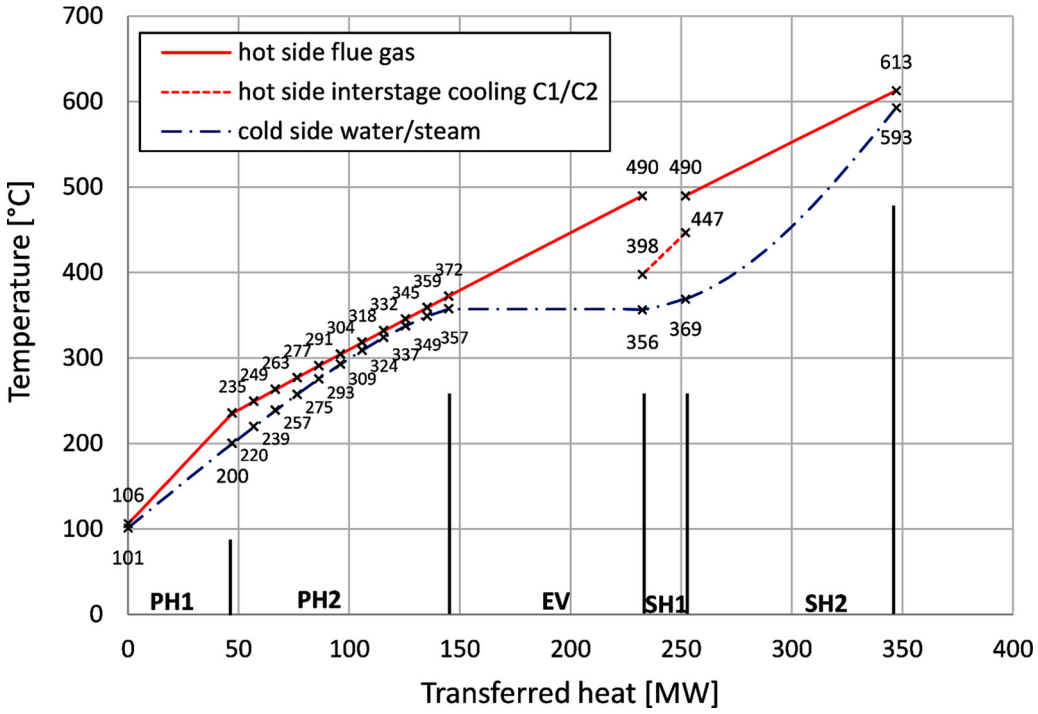

Fig. 8. Illustrative Q–T-diagram of the Graz Cycle.

zones of high and small temperature differences. The minimal allowed temperature differences in PH1, PH2 and EV, where liquid water is on the cold side, is set to 5 °C, whereas in SH1 and SH2 it is 20 °C. The pinch-point occurs at the cold inlet of PH1, inside PH2 the temperature difference does not fall below 5 °C.

3.3. ASU modelling

In the simulation models of both cycles the ASU is outside of the system boundaries. Its power consumption is thus considered with data from (IEAGHG, 2015) for the respective condition and composition of the oxygen stream.

For the NC oxygen with a purity of 99.5% (molar basis) at 120 bar and 15 °C is produced. For delivering oxygen at these conditions as well as supplying heat for the recuperator 1391 $kJ/kg_{oxygen\text{-}stream}$ are necessary according to (IEAGHG, 2015). This specific work multiplied with the mass flow rate of the oxygen stream results in the power consumption of the ASU as considered.

In the GC model oxygen is supplied with a purity of only 97% (molar basis) since according to (IEAGHG, 2015) this composition results in a maximum net efficiency. It is delivered at 16 bar and 15 °C, which results in a specific work of 1049 $kJ/kg_{oxygen\text{-}stream}$. The oxygen stream is then warmed up with heat from the CPU, compressed to 40 bar and fed to the combustion chamber at a temperature of 150 °C. A possible use of the cooling heat in the ASU as in the NC is not considered, but it might be a potential for improvement. The influence of the different oxygen purity on the cycle efficiency is discussed below in chapter 4.

3.4. CPU model

The separated CO_2 streams of both cycles are transferred to pipelines at a pressure of 110 bar and a temperature of 30 °C with a CO_2 purity of 99.6–99.8%. The power consumption for the CPU that is needed is taken from the data of (IEAGHG, 2015), where both cycles are analyzed. In this report a CO_2 capture rate of 90% is fulfilled, the rest of CO_2 leaves with the inert gas stream in the purification unit. A much higher capture rate could be achieved, if a lower purity were acceptable.

In the NC the separated CO_2 enters the CPU at 33 bar and 29 °C. According to (IEAGHG, 2015) 139.5 kJ/kg are necessary for the CPU, which is multiplied with the mass flow rate of the separated CO_2 stream to obtain the consumed power.

For the GC the power consumption of the compression from vacuum to 1 bar by the compressors C3 and C4 is included in the cycle efficiency, whereas the following compression and water removal with the compressors C5 and C6 to around 35 bar and 28 °C is assigned to the CPU efforts. The additional CPU starting at 35 bar requires 114.5 kJ/kg according to (IEAGHG, 2015)

3.5. Equation of state (EOS) model

Since there are limited flow properties available for mixtures of steam and CO_2 with other gases, simplified assumptions on the equation of state of these mixtures must be used, which, however, can have a considerable impact on the results. The EOS model implemented by the authors into IPSEpro is established as follows: The physical properties of water and steam are calculated using the IAPWS_IF97 formulations (Wagner and Kruse, 1998). CO_2 is modelled as real gas based on correlations of REFPROP (Lemmon et al., 2013). The small quantities of O_2, N_2 and Ar are calculated as ideal gases. The properties of the mixtures are calculated using Dalton's law of partial pressures, which is correct for ideal gases.

In order to evaluate the trustworthiness of the EOS used a comparison with the REFPROP data is performed (Kunz and Wagner model for hydrocarbon mixtures (Kunz et al., 2007)), which are considered as a standard. The comparison is done for the predicted powers of the main components (turbine, compressors and pumps) of the NC and the GC. For the NC the comparison in Table 1 shows deviations in the powers of the machines which result in a difference of the thermal cycle efficiency of 0.42%. For the conditions of the GC the data of IPSEpro and REFPROP match very well as shown in Table 2.

The comparison indicates the importance of the EOS model. But since too few experimental data are available for both cycle fluids, some uncertainty in the thermodynamic simulation must be accepted.

Table 1
Comparison of the predicted powers of the NET Power cycle for IPSEpro and REFPROP data.

NET Power cycle	IPSEpro	REFPROP	% deviation from REFPROP
Turbine power [MW]	619.10	620.95	−0.30%
Compressors power [MW]	61.85	60.98	1.42%
Pumps power [MW]	46.10	45.63	1.03%
Thermal cycle efficiency [%]	66.91%	67.33%	

Table 2
Comparison of the predicted powers of the Graz Cycle for IPSEpro and REFPROP data.

Graz Cycle	IPSEpro	REFPROP	% deviation from REFPROP
HTT power [MW]	625.12	625.05	0.01%
HPT power [MW]	46.55	46.55	0.00%
C1 and C2 power [MW]	203.14	203.15	−0.01%

3.6. Discussion of main parameters and assumptions

Natural gas is used as fuel with the same main properties and composition as in (IEAGHG, 2015) (see Table 3).

The cooling water temperature is assumed with 15 °C and allows cooling to minimal 26 °C as in (IEAGHG, 2015). The combustion is modelled as a complete chemical gross reaction with all educts reacting to products. An oxygen excess of 3% is prescribed in order to ensure a nearly complete combustion. Firing losses of 0.25% of the supplied heat, based on the lower heating value, are assumed.

Equivalent assumptions for the efficiencies of the respective components of both cycles are made and are summarized in Table 4. The aerodynamic losses due to the cooling flows in the cooled turbines are considered in their lower efficiencies. Attention is also paid to prescribe comparable pressure losses for both cycles. The values are listed in Table 5. For the HPT feed pipe a temperature loss of 5 °C is also considered.

The pinch point for the recuperator and the GC HRSG is determined with 5 °C as discussed above. Moreover, a minimal temperature difference at the outlet of the cold streams of the recuperator and the superheater 2 of the HRSG is assumed with 20 °C due to the gas-gas heat transfer.

Auxiliary losses (P_{aux}) are chosen with 0.35% of the supplied heat (based on the LHV) as in (Sanz et al., 2005).

The starting pressure for the dense phase compression of the NC is related to the cooling water temperature. This is set to 80 bar and 26 °C and the oxidant stream mass flow is determined assuming a molar fraction of oxygen of 13.34%, both according to (IEAGHG, 2015).

For the GC it is further assumed that the natural gas is preheated to 100 °C with heat available from the CPU. The outlet pressure of the HTT is slightly higher than 1 bar to minimize leakage in the following HRSG. The condensed water is compressed to 1 bar with a pump in front of the deaerator. The outlet temperature of the compressor C2 is limited to 600 °C so that the material stresses are not excessively high.

The number of stages of the cooled turbines has a considerable impact on the turbine coolant mass flow and therefore also on the simulation result. So a preliminary design of the cooled turbines is done before the cycle analysis. For the GC this was done in (Jericha et al., 2006). The GC HTT consists of two components, where the first one is free-running and drives the compressors C1 and C2, and the second one the generator at 3000 rpm. The layout resulted in one cooled transonic stage for the compressor turbine and two cooled and three uncooled stages for the power turbine.

No information is available in the literature about the number of cooled stages for the NC turbine. A rotational speed of 3000 rpm is assumed for the design to avoid the need for a generator drive gear box. Additional assumptions on the load coefficient with a value of 5, reaction ratio, the ratio of the mid diameter to blade length at inlet and outlet and the stator exit angle were made similar to the GC HTT turbine. These assumptions result in a turbine stage number of nine. Assuming a similar enthalpy drop per stage leads to six cooled and three uncooled stages.

Table 3
Composition and delivery condition of the natural gas.

Methane [vol%]	89
Ethane [vol%]	7
Propane [vol%]	1.11
CO_2 [vol%]	2
N_2 [vol%]	0.89
Lower heating value LHV [MJ/kg]	46.502
Temperature [°C]	15
Pressure [bar]	70

Table 4
Component efficiencies used in the thermodynamic simulation.

	NC	GC
Isentropic efficiency recycle compressors η_s	0.88	
Isentropic efficiency compressors C1/C2 η_s		0.88
Isentropic efficiency compressors to 1 bar C3/C4 η_s		0.85
Isentropic efficiency compressors from 1 bar to 35 bar C5/C6 η_s		0.85
Isentropic efficiency supercritical pumps η_s	0.85	
Isentropic efficiency pumps η_s		0.85
Isentropic efficiency turbine η_s	0.90	
Isentropic efficiency HTT η_s		0.90
Isentropic efficiency HPT η_s		0.90
Isentropic efficiency LPT η_s		0.88
Isentropic efficiency natural gas compressor η_s	0.81	
Isentropic efficiency O_2 compressor η_s		0.828
Mechanical efficiency η_m	0.99	0.99
Generator efficiency η_{gen}	0.985	0.985
Transformer efficiency η_{tr}	0.997	0.997

Table 5
Component pressure losses used in the thermodynamic simulation.

	NC	GC
Recuperator cold side	1%	
Recuperator hot side		
Turbine outlet stream	2%	
ASU air stream	0.2 bar	
Preheater 1		0.125%
Preheater 2		0.125%
Evaporator		0.125%
Superheater 2		0.125%
HRSG hot side (total)		0.5%
Preheater 1		1%
Preheater 2		1%
Evaporator		1%
Superheater 1		1%
Superheater 2		1%
HRSG cold side (total)		5%
Superheater 1 hot side		2%
Deaerator hot side		0.125%
Deaerator cold side		1%
HPT feed pipe		5 bar
Combustion chamber	2%	
Condenser	1%	
Intercooler hot side	2%	

4. Results and discussion of the base cases

The NC and the GC are investigated and compared at full load with an output power of 400 MW. Firstly, a base case for both cycles is

Table 6
Key cycle variables of NET Power cycle.

Parameter	Value
Combustion outlet temperature	1150 °C
Turbine inlet pressure	300 bar
Turbine outlet pressure	34 bar
Pressure in front of 1st pump	80 bar
Pressure in front of 2nd pump	120 bar

Table 7
Key cycle variables of Graz Cycle.

Parameter	Value
Combustion outlet temperature	1400 °C
HTT inlet pressure	40 bar
HTT outlet pressure	1.05 bar
Pressure after compressor C1	13.7 bar
Condenser pressure	0.07 bar
Pressure after compressor C4	1 bar
HPT inlet pressure	170 bar

modelled and investigated. For the NC the key cycle variables of (Scaccabarozzi et al., 2016) are used as reported in Table 6. The GC's key variables are based on the values from (Sanz et al., 2005) and are illustrated in Table 7.

The resulting power balances for the base cases are shown in Table 8.

The compressor power consumption for the GC is higher than for the NC, which is mainly due to the compressors C1 and C2. This is compensated, however, by the higher turbine power of the GC.

The NC needs additional power for compressing the natural gas (P_{fuel}) from the delivery condition of 70 bar to 300 bar whereas there is no power consumption needed for the GC. Furthermore, the GC requires less power for O_2 generation and compression. O_2 is delivered at a pressure of 120 bar to the NC, compared to 40.8 bar to the GC, and even the exhaust heat of the ASU (approx. 63 MW) can be used for the recuperator of the NC. For CO_2 purification and compression the power consumption is considerably lower for the NC as the compression of the CO_2 stream to 110 bar starts at 33 bar in comparison to 1 bar for the GC.

For the key cycle variables of the base case the NC shows a slightly better net efficiency with 52.4% toward the GC with 52.2% (for the efficiency definitions see Eq. (1) and Eq. (2)).

Table 8
Power balance for the base cases of the NET Power cycle and the Graz Cycle.

	NC	GC
Total heat input (Q_{in}) [MW]	763.94	766.44
Turbine power (P_T) [MW]	619.10	734.82
HTT [MW]		625.12
HPT [MW]		46.55
LPT [MW]		63.15
Recycle flow compressors ($P_{C,rec}$ (NC) or $P_{C1\text{-}C4}$ (GC)) + pumps (P_P) power consumption [MW]	103.26	219.93
Compressors C1 and C2 power [MW]		203.14
Fuel compressor power (P_{fuel}) [MW]	4.69	0.00
Net shaft power [MW] without mechanical losses	511.15	514.89
Thermal cycle efficiency [%]	**66.9%**	**67.2%**
Electrical power output [MW] incl. mechanical, electrical and auxiliary losses (P_{aux})	491.23	493.26
Net electrical cycle efficiency [%]	**64.3%**	**64.4%**
O_2 generation and compression (P_{ASU} or P_{ASU} + $P_{C,O2}$) [MW]	85.06	73.76
Efficiency considering O_2supply [%]	**53.2%**	**54.7%**
CO_2 compression and purification (P_{CPU} or P_{CPU} + P_{C5+6}) [MW]	6.16	19.29
Net power output [MW]	400.00	400.00
Net efficiency η_{net} [%]	**52.4%**	**52.2%**

Table 9
Influence of O_2 purity and CO_2 purification on the net efficiency.

Net efficiency η_{net} [%]	NC	GC
Base case	52.36%	52.19%
Base case with O_2 purity of 97%	52.21%	52.19%
Base case without CO_2 purification	52.72%	52.42%
Base case with O_2 purity of 97% and without CO_2 purification	52.57%	52.42%

$$\eta_{net,NC} = \frac{(P_T{*}\eta_m - \frac{\sum P_{C,rec}}{\eta_m}){*}\eta_{gen}{*}\eta_{tr} - \frac{\sum P_P}{\eta_m} - \frac{P_{fuel}}{\eta_m} - P_{aux} - P_{ASU} - P_{CPU}}{\dot{Q}_{in}} \quad (1)$$

$$\eta_{net,GC} = \frac{\left(\sum P_T{*}\eta_m - \frac{P_{C1+2}}{\eta_m}\right){*}\eta_{gen}{*}\eta_{tr} - \frac{P_{C3+4}}{\eta_m} - \frac{\sum P_P}{\eta_m} - P_{aux} - P_{ASU} - \frac{P_{C,O_2}}{\eta_m} - P_{CPU} - \frac{P_{C5+6}}{\eta_m}}{\dot{Q}_{in}} \quad (2)$$

In order to better understand the effect of the O_2 purity and the CO_2 purification on the net efficiency further investigations of the base case were carried out (see Table 9). Firstly, the NC was simulated with oxygen of the same purity as the GC (97%). This results in a slight decrease of 0.15% points in the net efficiency. Secondly, the effect of a CO_2 compression to 110 bar but without further purification on NC and GC were investigated. An increase in the net efficiency of 0.36% points for the NC and 0.23% points for the GC is observed. Thirdly, the base case with a O_2 purity of 97% and without CO_2 purification was simulated resulting in an increase of the net efficiency of the NC of 0.21% points and of the GC of 0.23% points. So if a lower CO2 purity is acceptable, e.g. for underground storage, more economic plants can be erected at slightly higher efficiencies.

In (Scaccabarozzi et al., 2016) the "efficiency considering O_2 supply" for the base case of the NC is 54.58%, compared to 53.17% in this work. Three factors are found for this difference of 1.41%-points:

- The isentropic efficiencies of the turbines and compressors and the pressure losses were assumed to be slightly different for a better comparability to the GC. However, this is beneficial, resulting in a higher efficiency of 0.15% points.
- In (Scaccabarozzi et al., 2016) a mechanical efficiency of 98% is considered compared to 99% in this work. Additionally, losses are considered for generator (98.5% efficiency) and the transformer (99.7%). This results in a reduction of the efficiency in this work of about 0.35% points.
- The first two points only explain an efficiency difference of about 0.2% points. The remaining 1.2% points are mainly caused by the different EOS models (in (Scaccabarozzi et al., 2016) the Peng-Robinson equation of state is used).

Due to its strong influence the EOS model will be further discussed. For the inlet and outlet conditions as well as fluid compositions given by (Scaccabarozzi et al., 2016) the resulting power for the cooled turbine and the compression is re-calculated in IPSEpro and in REFPROP (see Table 10). The turbine power is considerably lower for IPSEpro and REFPROP than in (Scaccabarozzi et al., 2016) indicating that the different EOS models result in different specific enthalpies at the turbine inlet and outlet. The compressor and pump power consumption is also lower for IPSEpro and REFPROP but there is still a considerable net power loss, which explains mainly the difference to the work of (Scaccabarozzi et al., 2016).

For the GC a comparison of the net efficiency of the base case of this work (52.19%) with the net efficiency in (IEAGHG, 2015) (49.4%) shows a considerable difference, although in (IEAGHG, 2015) a higher maximum temperature of 1533 °C and a higher maximum pressure of 46.5 bar compared to 1400 °C and 40 bar of this work were assumed.

Table 10
Comparison of the turbine, compressor and pump power of the NET Power cycle for different Equation of State models.

Base case of (Scaccabarozzi et al., 2016)	Mass flow rate [kg/s]	Temperature [°C]	Pressure [bar]
Turbine inlet	1271.00	1150.00	300.00
Turbine outlet	1370.40	741.18	34.00
Turbine cooling	99.40	183.00	303.00
	(Scaccabarozzi et al., 2016)	IPSEpro	REFPROP
Turbine power [MW]	622.42	600.94	595.19
Compressor and pump power [MW]	111.15	106.78	105.17
Turbine minus compressor and pump power [MW]	511.27	494.16	490.02

Table 11
Ratio of turbine cooling stream to turbine inlet stream and its impact on the net efficiency.

Ratio of turbine cooling stream to turbine inlet stream	This work	(IEAGHG, 2015)	Case 1	Case 2
HTT turbine 1	0.0425	0.1379	0.0677	0.1379
HTT turbine 2	0.0207	0.1116	0.0348	0.1116
Net efficiency [%]	52.19	49.4	53.69	50.64

The main difference is found to originate from the different cooled turbine models by investigating two more cases. Firstly, a case with increased maximum temperature and increased maximum pressure as in (IEAGHG, 2015) (case 1) and secondly additionally with increased turbine cooling stream (case 2) are simulated. Table 11 shows that for the base case and even for case 1 with a higher maximum temperature the ratio of turbine cooling stream to turbine inlet stream is significant lower than in (IEAGHG, 2015). If the same ratio of turbine cooling stream to turbine inlet stream as in (IEAGHG, 2015) is assumed (case 2), a reduction of the net efficiency of about 3% points in comparison to case 1 is predicted indicating the strong impact of the turbine cooling model.

As for the NC also for the GC a difference of the net efficiency is found to stem from the different EOS model by comparing the turbine powers. For the inlet and outlet conditions as well as fluid compositions given by (IEAGHG, 2015) the power of the turbines is re-calculated in IPSEpro and in REFPROP (see Table 12). There is a slight difference in the power of the HTT and the LPT but for the HPT the power in (IEAGHG, 2015) is significantly lower than for IPSEpro and REFPROP. This lower total turbine power of (IEAGHG, 2015) results in an additional reduction of the net efficiency by about 1%-point.

5. Parameter study

Starting from the base cases several main cycle parameters are varied to evaluate their impact on the net efficiency for a further optimization. As the parameters interact strongly, a multi-dimensional optimization is conducted below with the IPSEpro-PSOptimize-module (see chapter 6).

5.1. NET Power cycle

For the NC the influence of the parameters turbine inlet pressure, turbine outlet pressure and combustion outlet temperature is investigated.

Table 12
Comparison of the turbine powers of the Graz Cycle for different Equation of State models.

	(IEAGHG, 2015)	IPSEpro	REFPROP
HTT [MW]	1292.0	1297.0	1296.9
HPT [MW]	90.9	100.6	100.5
LPT [MW]	148.0	148.6	148.4
Total turbine power [MW]	1530.9	1546.2	1545.8

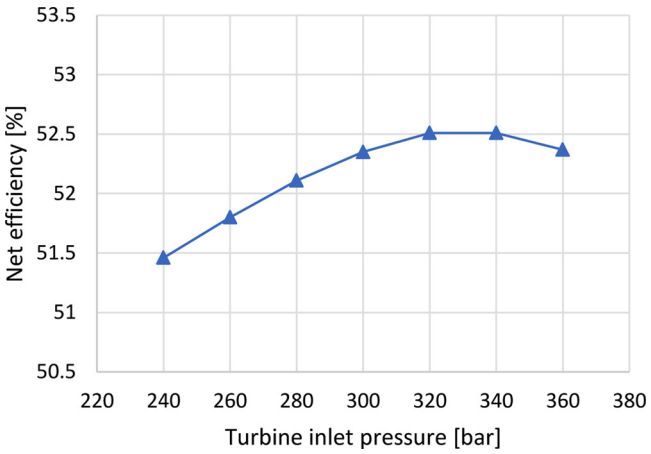

Fig. 9. Net efficiency as a function of turbine inlet pressure (NC).

5.1.1. Turbine inlet pressure

The turbine inlet pressure is varied from 240 bar to 360 bar while all other parameters and assumptions are kept constant. A maximum of the net efficiency is found between 320 bar and 340 bar (Fig. 9), however the change is small over the range of 300 bar – 360 bar (0.16%-points).

An interesting fact is that at the pressures between 340 bar and 360 bar the temperature difference at the outlet of the recuperator of 20 °C cannot be maintained and increases. At the same time the temperature difference at the inlet between the recycle stream and the turbine outlet stream increases too (Fig. 10). This means that the available heat from the turbine outlet stream is used less effectively, which also explains the net efficiency decrease in this range.

5.1.2. Turbine outlet pressure

For the turbine outlet pressure the value was varied between 28 bar and 42 bar. For increasing turbine outlet pressure the specific work of the turbine decreases but at the same time the specific work of the compressors also decreases. Moreover, a higher turbine outlet pressure is beneficial for the following compression of the CO_2 stream to 110 bar in the CPU.

The changes of the net efficiency in the investigated range are small (0.18%-points) (Fig. 11). However, it must be mentioned that the pressure ratio of the recycle compressors interact strongly with the turbine outlet pressure and should therefore be adapted, which is covered in chapter 6.

5.1.3. Combustion outlet temperature

On varying the combustion outlet temperature larger changes of the net efficiency arise (Fig. 12). A distinct optimum is achieved for a combustion outlet temperature of 1134 °C, which is found for a minimum temperature difference of 5 °C at the outlet of the cold streams of HX1 to the ASU air stream (Fig. 13). This temperature also results in a temperature difference just slightly above 5 °C between the

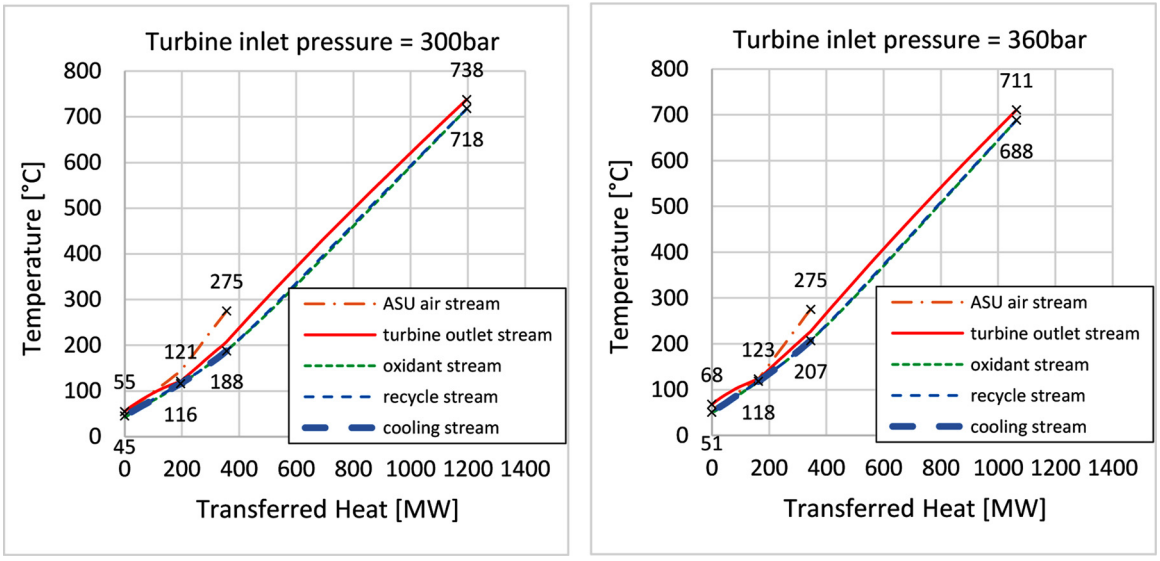

Fig. 10. Q-T diagram for a turbine inlet pressure of 300 bar (on the left) and 360 bar (on the right) (NC).

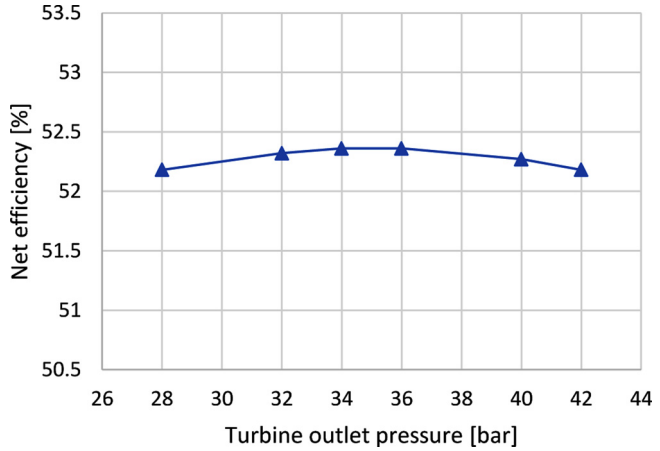

Fig. 11. Net efficiency as a function of turbine outlet pressure (NC).

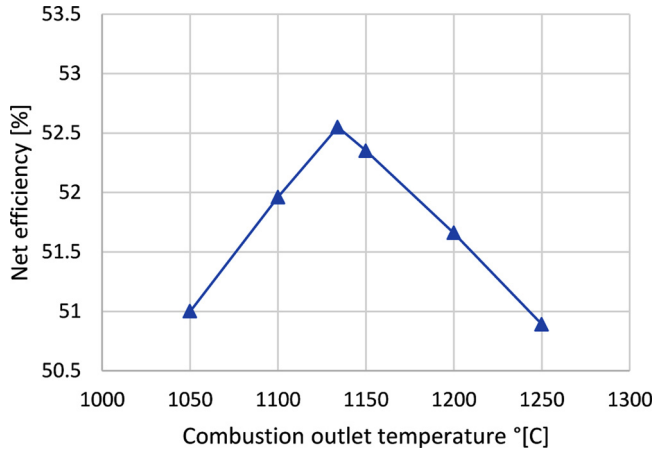

Fig. 12. Net efficiency as a function of combustion outlet temperature (NC).

turbine outlet stream and the recycle stream at the inlet of the cold streams of HX1, which means optimal use is made of the exhaust heat.

5.2. Graz Cycle

The cycle parameters combustion outlet temperature, HTT inlet pressure, HPT inlet temperature, HPT inlet pressure, condenser pressure as well as the intermediate pressure of the compressors C1/C2, C3/C4 and C5/C6 are investigated for the GC.

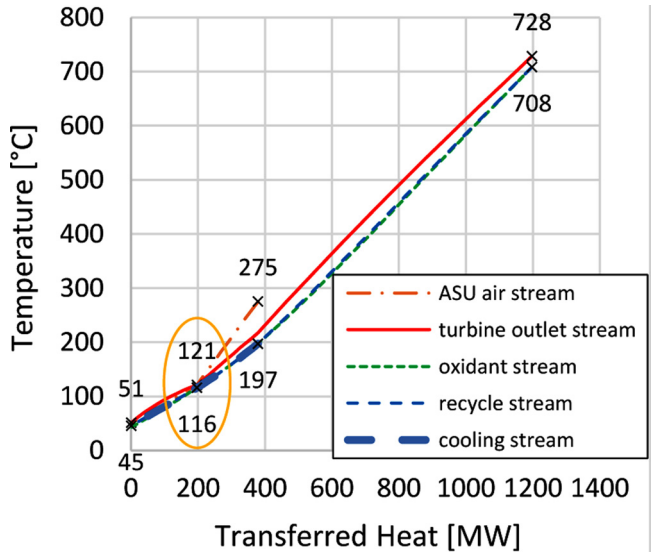

Fig. 13. Q-T diagram for optimal combustion outlet temperature (NC).

5.2.1. Combustion outlet temperature

The net efficiency increases considerably with higher combustion outlet temperatures, as shown in Fig. 14. This can be explained by the higher mean temperature of the heat input, which results in higher efficiencies according to Carnot. The maximum temperature is limited to 1500 °C. For a constant fuel mass flow a temperature rise from 1250 °C to 1500 °C results in considerably decreasing mass flows at the HTT inlet and the compressors C1/C2 (see Fig. 15), which, in turn, result in decreasing turbine and compressor powers of Fig. 14.

5.2.2. HTT inlet pressure

The same positive effect is found for increasing HTT inlet pressure (see Fig. 16). But the effect is less, because the power consumption of the compressors C1 and C2 as well as of the pumps increases for higher pressures. The maximum pressure is limited to 50 bar.

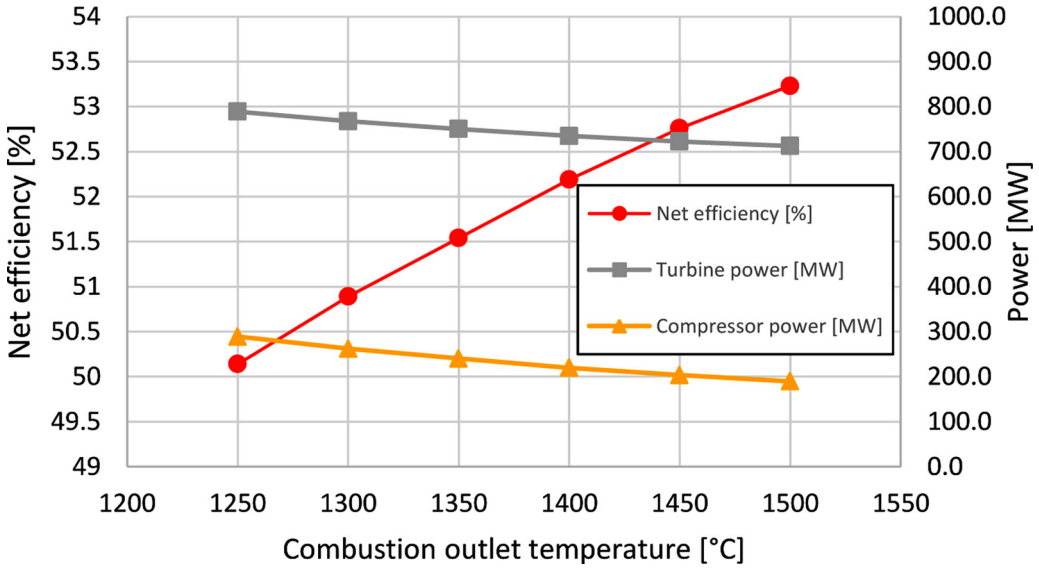

Fig. 14. Net efficiency, turbine and compressor power as a function of combustion outlet temperature (GC).

5.2.3. HPT inlet temperature

Higher inlet temperatures of the HPT also result in higher net efficiencies as illustrated in Fig. 17. For lower HPT inlet temperatures the temperature difference at the outlet of the HRSG is considerably higher than 20 °C und therefore the full potential of the HRSG is not exploited (see Fig. 18). However, part of that effect is compensated as the H_2O content of the cycle fluid increases and therefore the mass flow rate of the compressors C1 and C2 and their power consumption decreases.

The HPT inlet temperature is limited to 600 °C due to material reasons. In the base case only 583 °C is reached because of the required minimal temperature difference of 20 °C at the HRSG outlet and a further 5 °C temperature drop in the feed steam line.

5.2.4. HPT inlet pressure and intermediate pressure between compressors C1 and C2 as well as C3 and C4

The net efficiency increases almost linearly with a higher HPT inlet pressure from 51.79% for a pressure of 120 bar to 52.19% for 170 bar. As the steam cycle is subcritical a pressure of 170 bar is set as maximum pressure.

In the context of the intermediate pressure of the cycle compressors C1 and C2 the net efficiency increases slightly for decreasing values, as for the base case the pressure ratio of the compressor C1 is considerably higher than that of the compressor C2. A lower intermediate pressure leads to a reduced outlet temperature of compressor C1, which is limited by a required minimum temperature difference of 20 °C at the outlet of the hot side of SH1. Therefore, the intermediate pressure is limited to 12.01 bar, which gives the best net efficiency with 52.21%.

For the compressors C3 and C4, which compress the CO_2 stream to 1 bar, a maximum of the net efficiency is found for the intermediate pressure between 0.15 bar and 0.25 bar. By varying this pressure from 0.1 bar to 0.4 bar an improvement by 0.25% points can be achieved.

5.2.5. Condenser pressure

A lower condenser pressure results in a higher power of the LPT, but on the other hand the amount of separated water is reduced, which leads to a higher mass flow rate and thus higher power demand of the compressor C3. Therefore for a minimum cycle temperature of 26 °C an optimum condenser pressure exists between 0.06 bar and 0.07 bar as illustrated in Fig. 19.

6. Cycle optimization

Since the investigated cycle parameters interact strongly, a further multi-dimensional optimization was carried out with the IPSEpro-PSOptimize-module. This tool uses a genetic algorithm in which ranges for several parameters are defined and a maximum (or minimum) for a

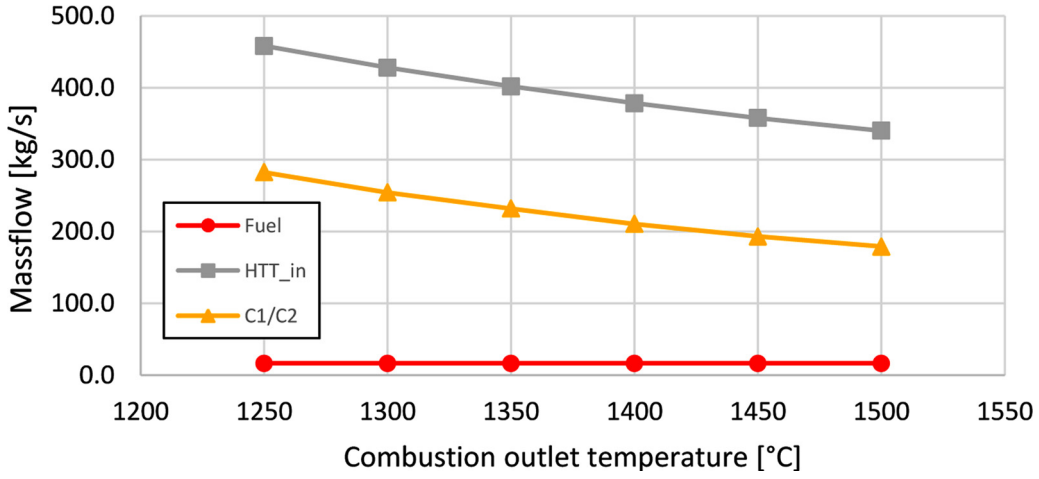

Fig. 15. Mass flow at HTT inlet and compressors C1/C2 at constant fuel mass as a function of combustion outlet temperature (GC).

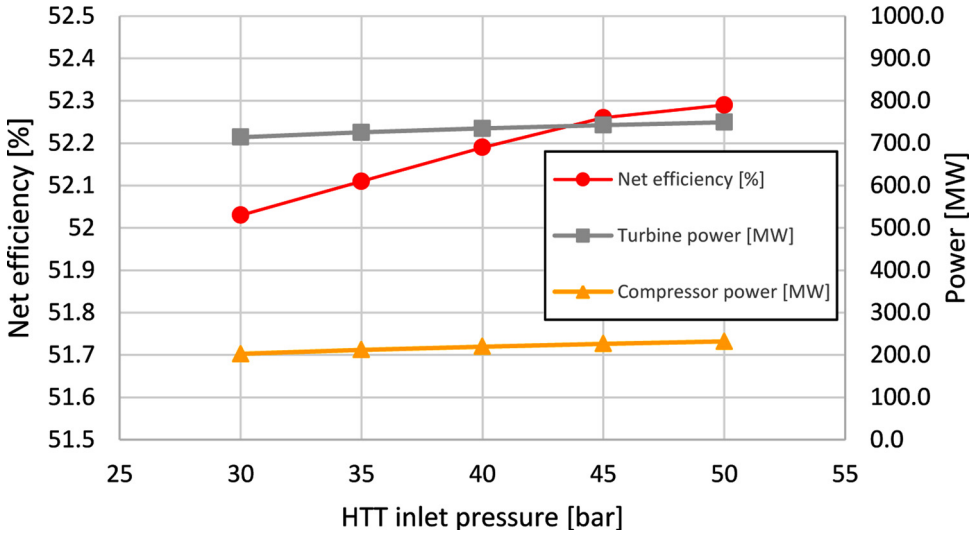

Fig. 16. Net efficiency, turbine and compressor power as a function of HTT inlet pressure (GC).

prescribed function are searched for, and the function in this case is the net efficiency.

The investigated parameters and their ranges are chosen based on the analysis of the parameter study in chapter 5 as well as on the analysis of (Scaccabarozzi et al., 2016) and are found in Table 13 and Table 14.

For the NC the pressure ratio of the third recycle compressor is set so that in front of the fourth recycle compressor the CO_2 is at its saturation curve in order to avoid it getting into the wet steam region.

Through the analysis of sub-chapter 5.2 it is found for the GC that for the parameters combustion outlet temperature, HTT inlet pressure, HPT inlet temperature and HPT inlet pressure the maximum of the net efficiency is obtained at their highest possible values. These values are thus set. For the HPT inlet temperature the highest temperature is reached by setting the temperature difference at the outlet of the cold side of SH2 to 20 °C. For the intermediate pressure of C1/C2 the best value (concurrent with the minimal possible pressure) is obtained by setting the temperature difference at the outlet of the hot side of superheater 1 to 20 °C.

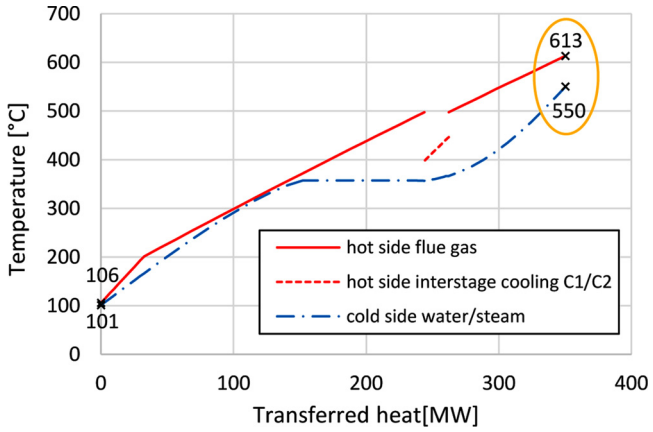

Fig. 18. Q-T diagram for an HPT inlet temperature of 545 °C (GC).

6.1. Results of cycle optimization

The cycle data for the optimized NC are presented in Table 15. An increase of the net efficiency of 0.36% points is achieved. Although the

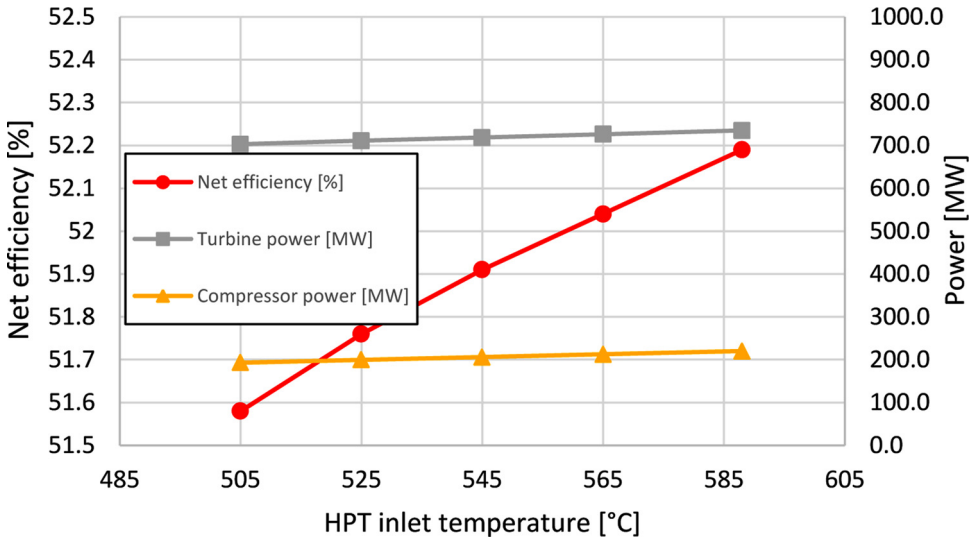

Fig. 17. Net efficiency, turbine and compressor power as a function of HPT inlet temperature (GC).

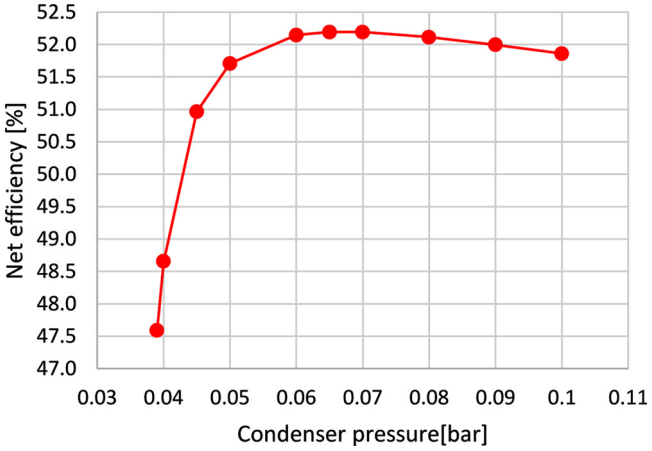

Fig. 19. Net efficiency as a function of condenser pressure (GC).

Table 13
Parameters and their ranges for the optimization of the NET Power cycle.

Parameter	Parameter range
Turbine inlet pressure	290 – 360 bar
Turbine outlet pressure	28 – 50 bar
Combustion outlet temperature	1050 – 1250 °C
Pressure ratio of recycle compressor 1 and 2	1.05 – 1.5

Table 14
Parameters and their ranges for the optimization of the Graz Cycle.

Parameter	Parameter range
Combustion outlet temperature	1500 °C
HTT inlet pressure	50 bar
HPT inlet temperature	Maximal possible temperature (limit: 600 °C)
HPT inlet pressure	170 bar
C1/C2 intermediate pressure	Minimal possible pressure
Condenser pressure	0.05 – 0.07 bar
C3 pressure ratio	2 – 6
C5 pressure ratio	4 – 8

Table 15
Key cycle data of the optimized NET Power cycle in comparison to its base case.

	Base case	Optimized
Turbine inlet pressure [bar]	300	317.94
Turbine outlet pressure [bar]	34	46.44
Combustion outlet temperature [°C]	1150	1120.45
Recycle compressor 1 pressure ratio	1.3	1.26
Recycle compressor 2 pressure ratio	1.3	1.13
Net power output [MW]	400	400
Net efficiency [%]	52.36	52.72
Total heat input (Q_{in}) [MW]	763.94	758.79
Turbine power (P_T) [MW]	619.10	607.32
Recycle flow compressors ($P_{C,rec}$) + pumps power (P_P) [MW]	103.26	92.59
O_2 generation & compression (P_{ASU}) [MW]	85.06	84.48
CO_2 compression and purification (P_{CPU}) [MW]	6.16	5.56
Discharged heat to cooling water [MW]	365.66	358.62
Specific work [MJ/kg]	0.32	0.29
Volume specific work [MJ/m^3]	32.04	31.08
Turbine outlet temperature [°C]	737.91	755.51
Temperature recycle stream after recuperator [°C]	717.91	735.51
Temperature cooling stream after recuperator [°C]	187.80	204.72
Temperature turbine outlet stream after recuperator [°C]	55.04	52.29
Temperature recycle stream in front of recuperator [°C]	45.39	47.01
Turbine inlet flow rate [kg/s]	1257.6	1402.45
Cooling stream flow rate [kg/s]	89.58	92.55

Table 16
Key cycle data of the optimized Graz Cycle in comparison to its base case.

	Base case	Optimized
Combustion outlet temperature [°C]	1400	1500
HTT inlet pressure [bar]	40	50
HPT inlet temperature [°C]	587.83	599.04
HPT inlet pressure [bar]	170	170
C1/C2 intermediate pressure [bar]	13.7	15.02
Condenser pressure [bar]	0.07	0.0633
C3 pressure ratio	3.61	2.63
C5 pressure ratio	5.86	6.73
Net power output [MW]	400	400
Net efficiency [%]	52.19	53.49
Total heat input (Q_{in}) [MW]	766.44	747.73
Turbine power (P_T) [MW]	734.82	710.32
HTT [MW]	625.12	610.71
HPT [MW]	46.55	40.53
LPT [MW]	63.15	59.08
Recycle flow compressors ($P_{C1–C4}$) + pumps power (P_P) [MW]	219.93	196.86
Compressors C1 and C2 power [MW]	203.14	179.43
O_2 generation and compression (P_{ASU}) [MW]	73.76	73.28
CO_2 compression and purification (P_{CPU}) [MW]	19.29	18.88
Discharged heat to cooling water [MW]	353.70	333.98
Specific work [MJ/kg]	1.06	1.21
Volume specific work [MJ/m^3]	6.45	8.73
Turbine inlet flow rate [kg/s]	378.35	331.18
Cooling stream flow rate [kg/s]	24.25	30.24
Recycle stream flow rate [kg/s]	210.29	174.41
Steam flow rate [kg/s]	111.86	108.44

turbine power decreases, mainly due to the lower combustion temperature and higher turbine outlet pressure, this is compensated by a lower compression power, which is a result of the higher turbine outlet pressure and the optimized pressure ratios.

The increase of the net efficiency is also indicated by the lower discharged heat levels. On the one hand this is a result of the higher turbine outlet pressure and the optimized compressor ratios so that less heat is discharged in the compressor intercoolers. On the other hand it is a result of the good utilization of the exhaust heat in the recuperator. The turbine outlet stream exits the recuperator with a temperature of 52 °C and the temperature difference to the recycle and cooling stream is with 5.3 °C very close to its minimum of 5 °C (see Fig. 6 for comparison).

A further effect of the optimization is a decrease of the mass and volume specific work, which is the ratio of net power output to the turbine inlet mass or volume flow, respectively. This leads to larger components for the same power output.

For the GC partly similar effects are perceived (see Table 16). The increase of the net efficiency is larger with 1.30% points and stems mainly from the higher combustion outlet temperature (approx. 1.1%-points). The higher combustion outlet temperature also results in a higher temperature of the flue gas at the HRSG inlet which again results in a higher HPT inlet temperature of 599 °C (almost the maximum temperature of 600 °C).

Less turbine power is necessary for producing 400 MW as the compression power consumption also decreases. Both decreases are a result of smaller mass flows. For the turbine this is partly compensated by the higher inlet temperature and pressure. Moreover, the smaller mass flows result in a decrease of discharged heat in the condenser and intercoolers but also in an increase of the mass and volume specific work.

6.2. Comparison of the optimized cycles

Table 17 shows the comparison of the power balances for both optimized cycles. The thermal efficiency is higher for the GC with

Table 17
Power balance for the optimized NET Power cycle and the optimized Graz Cycle.

	NC	GC
Total heat input (Q_{in}) [MW]	758.79	747.73
Turbine power (P_T) [MW]	607.32	710.32
Recycle flow compressors ($P_{C,rec}$ (NC) or $P_{C1\text{-}C4}$ (GC)) + pumps (P_P) power consumption [MW]	92.59	196.86
Fuel compressor power (P_{fuel}) [MW]	4.87	0.00
Net shaft power [MW] without mechanical losses	509.86	513.46
Thermal cycle efficiency [%]	**67.2%**	**68.7%**
Electrical power output [MW] incl. mechanical, electrical & auxiliary losses	490.04	492.38
Net electrical cycle efficiency [%]	**64.6%**	**65.9%**
O_2 generation & compression (P_{ASU} or $P_{ASU}+P_{C,O2}$) [MW]	84.48	73.28
Efficiency considering O_2 supply [%]	**53.5%**	**56.0%**
CO_2 compression and purification (P_{CPU} or $P_{CPU}+P_{C5+6}$) [MW]	5.56	18.88
Net power output [MW]	400.00	400.00
Net efficiency η_{net} [%]	**52.7%**	**53.5%**

68.7% to 67.2% for the NC. As the GC has higher turbine and compressor powers the effect of the mechanical efficiency is stronger and so the difference is just 1.3% points for the net electrical efficiency. For the NC more power is needed for O_2 generation and less for the CO_2 compression and purification as mentioned in chapter 4. This results in a higher net efficiency for the GC with 53.5% to 52.7% for the NC.

The NC and the GC are very different from a thermodynamic perspective. For a better understanding of their advantages and disadvantages several cycle data are summarized and compared for both cycles in Table 18.

The main difference is the composition of the flue gas. For the NC CO_2 is the dominating part whereas for the GC it is H_2O. Moreover, the GC has a cycle part of Rankine type which is operated with pure water. Quite different fluid properties and cycle data are the consequence. The NC thus operates in the supercritical and gaseous area while the GC operates in the gaseous and two-phase region.

Although the NC has a higher combustion pressure, the turbine pressure ratio is lower (NC turbine pressure ratio: 6.85, GC turbine pressure ratio HTT: 47.62, LPT:16.58). The combustion temperature is considerably higher for the GC.

The lower turbine pressure ratio is one reason why the NC needs a higher mass flow rate after the combustion chamber, which results in a remarkably lower specific work of 0.29 MJ/kg compared to 1.21 MJ/kg for the GC. However, due to the high pressure and thus density of the cycle medium in the NC, the volume flow rate is smaller, so that the volume specific work of the NC is about 3.5 times larger. This allows a remarkably more compact design of the components, although lower efficiencies of the turbomachinery can be expected due to the smaller dimensions.

Table 18
Comparison of several cycle data of the NET Power cycle and the Graz Cycle.

	NC	GC
Composition after combustion chamber		
Ar [kg/kg]	0.51	0.90
CO_2 [kg/kg]	96.24	24.85
H_2O [kg/kg]	2.38	73.26
N_2 [kg/kg]	0.74	0.45
O_2 [kg/kg]	0.13	0.54
Turbine or HTT inlet pressure [bar]	317.94	50
Turbine or HTT inlet temperature [°C]	1120.45	1500
Turbine pressure ratio	6.85	
HTT		47.62
LPT		16.58
Mass flow rate after combustion chamber [kg/s]	1402.45	331.18
Volume flow rate [m^3/s]	12.87	45.82
Specific work [MJ/kg]	0.29	1.21
Volume specific work [MJ/m^3]	31.08	8.73
Recuperator and HRSG		
Transferred heat [MW]	1364.94	340.03
Pressure cold side [bar]	327.57	184.15
Pressure hot side [bar]	46.44	1.05
Utilized ASU exhaust heat [MW]	62.29	

In the recuperator the pressure differences between the hot and cold side are remarkably higher than in the HRSG. Moreover, considerably more power is transferred and the temperature at the inlet is above 700 °C. These circumstances make the design and manufacturing of the recuperator a relatively challenging task.

Another significant difference is that exhaust heat from the ASU is utilized for the NC.

In the context of the cycle structure the GC is more complex, as it has a recycle stream and an additional water/steam stream with three turbines altogether, whereas the NC has only one loop with one single turbine. This might result in an easier design and operation of the NC.

In order to assess the economic issues, the power of the turbomachinery components and heat exchangers is first compared since the costs are related to the power of the components. Table 17 shows that the GC needs 17% more turbine power and 113% more compression power, since in the NC compression is partly done by pumps. On the other hand, the transferred heat is by 301% higher in the NC (Table 18), where most heat is exchanged in the challenging recuperator. The complex recuperator leads in (IEAGHG, 2015) to direct material specific costs of the power island of 312 €/kW for the NC compared to 329 €/kW for the GC related to the net power output. In their study the total direct material costs including power island, ASU, CPU as well as utility units sum up to 680 €/kW for the NC and 777 €/kW for the GC, so that a slight economic advantage was found for the NC.

An optimization and investigation of the NC was also done with a more conservative preliminary turbine design from sub-chapter 3.6, which resulted in ten turbine stages, divided in seven cooled and three uncooled stages, thus one more cooled stage than before. This turbine design results in an increase of the cooling stream from 92.55 kg/s to 101.98 kg/s. The net efficiency decreases by 0.66% points to 52.06% due to the increase of the number of cooled stages. This means that the number of cooled stages and the underlying preliminary turbine design have a considerable effect on the net efficiency.

6.3. Influence of modified basic assumptions

In sub-chapter 3.6 assumptions for the machine efficiencies, the pressure losses and the minimal cycle temperature were made. This subchapter analyses the effects of modified assumptions.

Three cases are analyzed. In the first case all machine efficiencies are decreased by 5%-points. In the second case pressure losses that are twice as high for the heat exchangers and the combustion chamber are assumed. The third case analyses the effect of a minimal cycle temperature of 21 °C (corresponding to a cooling water temperature of 10 °C) to include regions where cooling water at lower temperatures is available. After this modification all cases are optimized as described in chapter 6. The results for these cases are presented in Fig. 20.

Lower efficiencies have a stronger impact on the GC than on the NC. The net efficiency of the GC decreases by 3.10% points to 50.39%, the net efficiency of the NC decreases by 2.43% points to 50.29%. The effect for the GC is higher as this cycle has higher turbine, compressor and pump powers.

Opposite effects are obtained when the pressure losses are doubled. This has a considerably stronger effect on the NC with a decrease in the net efficiency of 1.36% points in comparison to the GC with a decrease of 0.29% points. For the NC the higher pressure losses result in considerably higher power demands of the recycle compressors and the pumps whereas for the GC the higher pressure losses mainly affects the water stream which has a low pump power consumption.

Lower minimal cycle temperatures result in an increase of 0.24%

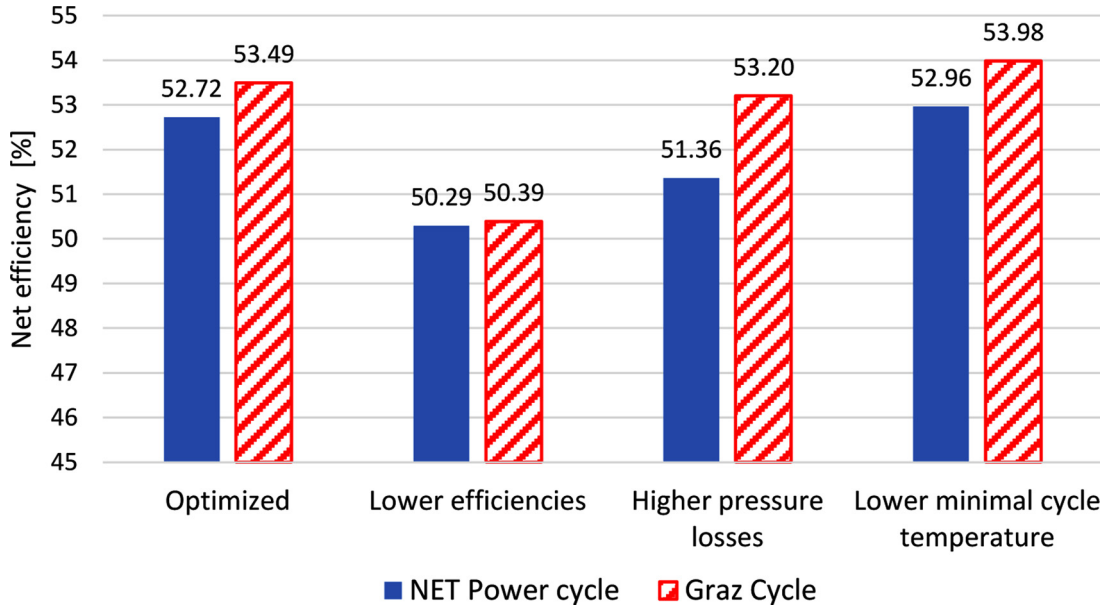

Fig. 20. Effect of modified assumptions on the net efficiency.

points for the NC and 0.49% for the GC. The increase for the NC is explained due to the better intercooling of the compressors. For the GC the lower minimal cycle temperature results in a lower condenser pressure and therefore back pressure for the LPT, so that it produces more power.

7. Conclusions

This work presents a thermodynamic comparison of the NET Power cycle with the Graz Cycle, two promising oxy-combustion cycles featuring nearly 100% CO_2 capture rate, including their modelling, analysis and optimization, in order to give advice, which cycle offers more potential for future applications. Another objective is to elucidate the influence of simulation tools, fluid property models and cycle parameters chosen on the conclusions which can be drawn from a thermodynamic study. Therefore a comparison with the exhaustive study by (IEAGHG, 2015) is also done.

Based on the cycle data of (Scaccabarozzi et al., 2016) for the NET Power cycle and of (Sanz et al., 2005) for the Graz Cycle a base case of each cycle is simulated, where similar assumptions on component efficiencies and losses are made for a reliable comparison. It resulted in net efficiencies of 52.4% for the NET Power cycle and 52.2% for the Graz Cycle. The lower efficiency of the NET Power cycle in this work compared to the 54.58% of the base case of (Scaccabarozzi et al., 2016) results mainly from different Equation of State models used and the fact that (Scaccabarozzi et al., 2016) did not take into account the power for the CO_2 compression and purification. The considerable difference in the net efficiency of the Graz Cycle to the results obtained in (IEAGHG, 2015) with 49.4% mainly stem from a different turbine model, from different Equation of State models, and different assumptions for component efficiencies and pressure losses.

In a further step the two cycles are optimized for maximum net efficiency by conducting a parameter study and a multi-dimensional optimization using the IPSEpro-PSOptimize-module. The increase of the net efficiency of the NET Power cycle by 0.36% points to 52.7% is mainly obtained by optimizing the turbine inlet temperature for optimal operation of the recuperator. One more interesting fact is that a pressure of 318 bar is optimal and higher values are disadvantageous as the recuperator works in a less efficient way. Moreover, the turbine outlet pressure in connection with the pressure ratios of the recycle compressors is optimized.

The optimization for the Graz Cycle results in an increase of the net efficiency of 1.30% points to 53.5%. Around 1.1% points increase can be related to the rise of the High Temperature Turbine inlet temperature from 1400 °C to 1500 °C. For the High Temperature Turbine inlet pressure (50 bar), the High Pressure Turbine inlet temperature (599 °C) and pressure (170 bar) the maximal possible values are found optimal but their effect on the net efficiency is considerably lower. Moreover, the condenser pressure and the intermediate pressures of the three compressor pairs are optimized.

The following results are obtained for the optimized cases:

- The comparison of the net efficiency shows a slight advantage for the Graz Cycle with 53.5% to 52.7% for the NET Power cycle.
- A more conservative preliminary turbine design of the NET Power cycle, which results in one more cooled turbine stage, decreases the net efficiency to 52.06%. This shows the need for an optimized turbine design.
- Lower machine efficiencies (minus 5%-points) have a stronger effect on the Graz Cycle than on the NET Power cycle, whereas higher pressure losses (doubled pressure losses in the heat exchangers and in the combustion chamber) are more critical for the NET Power cycle. Here the net efficiency for the Graz Cycle is considerably higher with 53.20% to 51.36% for the NET Power cycle.
- A reduction of the minimal cycle temperature from 26 °C to 21 °C affects the Graz Cycle slightly more positively.

Apart from the net efficiency the Graz Cycle has the advantage of a higher volume flow rate at the inlet of the High Temperature Turbine compared to the inlet of the turbine of the NET Power cycle which is beneficial for the turbine and thus for cycle efficiency, but on the other hand, the NET Power cycle components can be built in a more compact way. Moreover, comparing the recuperator (NET Power cycle) and the Heat Recovery Steam Generator (Graz Cycle), the recuperator is a considerably more challenging component with high pressure differences and high transferred thermal power. However, the NET Power cycle has a simpler cycle structure and needs fewer components, which might make its design and operation easier.

Regarding the second research question on the reliability of thermodynamic comparisons, this study shows that an advantage of 5.7% points in cycle efficiency can turn into a slight disadvantage if different simulation tools and models are used. Further investigations to find

reliable Equation of State models for working fluids of this kind are thus strongly recommended.

Funding

No funding was received for this work.

Intellectual property

We confirm that we have given due consideration to the protection of intellectual property associated with this work and that there are no impediments to publication, including the timing of publication, with respect to intellectual property. In so doing we confirm that we have followed the regulations of our institutions concerning intellectual property.

Research ethics

We further confirm that any aspect of the work covered in this manuscript that has involved human patients has been conducted with the ethical approval of all relevant bodies and that such approvals are acknowledged within the manuscript.

Authorship

We confirm that the manuscript has been read and approved by all named authors.

We confirm that the order of authors listed in the manuscript has been approved by all named authors.

Contact with the editorial office

Someone other than the Corresponding Author declared above submitted this manuscript from his/her account in EVISE:

We understand that this author is the sole contact for the Editorial process

CRediT authorship contribution statement

Kevin Wimmer: Methodology, Validation, Investigation, Data curation, Writing - original draft, Writing - review & editing, Visualization. **Wolfgang Sanz:** Conceptualization, Methodology, Writing - original draft, Writing - review & editing, Visualization.

Declaration of Competing Interest

No conflict of interest exists.

Appendix A. Supplementary data

Supplementary material related to this article can be found, in the online version, at doi:10.1016/j.ijggc.2020.103055.

References

Allam, R.J., Palmer, M., Brown, G.W., 2011. System and method for high efficiency power generation using a carbon doxde circulating working fluid. Patent US 2011/0179799 A1,2011.

Allam, R.J., Palmer, M.R., Brown, G.W., Fetvedt, J., Freed, D., Nomoto, H., Itoh, M., Okita, N., Jones, C., 2013. High efficiency and low cost of electricity generation from fossil fuels while eliminating atmospheric emissions, including carbon dioxide. Energy Proced. 37, 1135–1149. https://doi.org/10.1016/j.egypro.2013.05.211.

Allam, R., Martin, S., Forrest, B., Fetvedt, J., Lu, X., Freed, D., Brown, G.W., Sasaki, T., Itoh, M., Manning, J., 2017. Demonstration of the allam cycle: an update on the development status of a high efficiency supercritical carbon dioxide power process employing full carbon capture. Energy Proced. 114, 5948–5966. https://doi.org/10.1016/j.egypro.2017.03.1731.

Chiesa, P., Macchi, E., 2004. A thermodynamic analysis of different options to break 60% electric efficiency in combined cycle power plants. J. Eng. Gas Turbines Power 126, 770–785. https://doi.org/10.1115/1.1771684.

El-Masri, M.A., 1986. On thermodynamics of gas-turbine cycles: part 2—a model for expansion in cooled turbines. J. Eng. Gas Turbines Power 108, 151–159. https://doi.org/10.1115/1.3239862.

Fischedick, M., Görner, K., Thomeczek, M., 2015. Einleitung. CO2: Abtrennung, Speicherung, Nutzung - Ganzheitliche Bewertung Im Bereich Von Energiewirtschaft Und Industrie (in German). Springer-Verlag, Berlin, Heidelberg. https://doi.org/10.1007/978-3-642-19528-0.

Hartfield, G., Blunden, J., Arndt, D.S., 2018. State of the climate in 2017. Bull. Am. Meteorol. Soc. 99https://doi.org/10.1175/2018BAMSStateoftheClimate.1. Si-S310.

IEAGHG, 2015. Oxy-Combustion Turbine Power Plants, 2015/05, August, 2015.

International Energy Agency, 2016. World energy outlook 2016, world energy outlook. OECDhttps://doi.org/10.1787/weo-2016-en.

Jericha, H., 1985. Efficient steam cycles with internal combustion of hydrogen and stoichiometric oxygen for turbines and piston engines. CIMAC Conf. Pap., Oslo 1985.

Jericha, H., Sanz, W., Woisetschläger, J., Fesharaki, M., 1995. CO2 - retention capapility of CH4/O2 - fired Graz cycle. CIMAC Conf. Pap.

Jericha, H., Sanz, W., Göttlich, E., 2006. Design concept for large output graz cycle gas turbines. ASME pap. GT2006-90032. J. Eng. Gas Turbines Power. https://doi.org/10.1115/1.2747260.

Jericha, H., Sanz, W., Göttlich, E., Neumayer, F., 2008. Design Details of a 600 MW Graz Cycle Thermal Power Plant for CO2 Capture. ASME Pap. GT2008-50515. ASME Turbo Expo 2008https://doi.org/10.1115/gt2008-50515.

Jordal, K., Bolland, O., Klang, Å., 2003. Aspects of Cooled Gas Turbine Modelling for the Semi-closed O2/CO2 Cycle With CO2 Capture. ASME Pap. GT2003-38067. ASME Turbo Expo 2003https://doi.org/10.1115/gt2003-38067.

Kunz, O., Klimeck, R., Wagner, W., Jaeschke, M., 2007. The GERG-2004 wide-range equation of state for natural gases and other mixtures, GERG technical monograph 15. Fortschr.-Ber. VDI.

Lemmon, E.W., Bell, I.H., Huber, M.L., McLinden, M.O., 2013. NIST Standard Reference Database 23: Reference Fluid Thermodynamic and Transport Properties-REFPROP, Version 9.1. Natl. Inst. Stand. Technol. Stand. Ref. Data Progr.

Peng, D.Y., Robinson, D.B., 1976. A new two-constant equation of state. Ind. Eng. Chem. Fundam. 15, 59–64. https://doi.org/10.1021/i160057a011.

Sanz, W., Jericha, H., Moser, M., Heitmeir, F., 2004. Thermodynamic and Economic Investigation of an Improved Graz Cycle Power Plant for CO2 Capture. ASME Pap. GT2004-53722. ASME Turbo Expo 2004https://doi.org/10.1115/gt2004-53722.

Sanz, W., Jericha, H., Luckel, F., Gottlich, E., Heitmeir, F., 2005. A Further Step Towards a Graz Cycle Power Plant for CO2 Capture. ASME Pap. GT2005-68456. ASME Turbo Expo 2005https://doi.org/10.1115/GT2005-68456.

Sanz, W., Jericha, H., Bauer, B., Göttlich, E., 2008. Qualitative and quantitative comparison of two promising OXY-fuel power cycles for CO2capture. ASME Pap. GT2007-27375. J. Eng. Gas Turbines Power 130 (May (3)). https://doi.org/10.1115/1.2800350. 031702 (11 pages).

Scaccabarozzi, R., Gatti, M., Martelli, E., 2016. Thermodynamic analysis and numerical optimization of the NET Power oxy-combustion cycle. Appl. Energy 178, 505–526. https://doi.org/10.1016/j.apenergy.2016.06.060.

Scaccabarozzi, R., Gatti, M., Martelli, E., 2017. Thermodynamic optimization and part-load analysis of the NET power cycle. Energy Proced. 114, 551–560. https://doi.org/10.1016/j.egypro.2017.03.1197.

SimTech Simulation Technology, 2017. “IpsePro Overview”. http://www.simtechnology.com/IPSEpro.

Wagner, W., Kruse, A., 1998. Properties of Water and Steam. Springer-Verlag, Berlin Heidelberg.